Electronic Supplementary Material (ESI) for Journal of Materials Chemistry A.

Supporting Information

A Green-Low-Cost Rechargeable Zn-ion Aqueous Battery Using Hollow Porous Spinel $ZnMn_2O_4$ as the Cathode Material

Xianwen Wu [a, b, c*], Yanhong Xiang [a], Qingjing Peng [a, b, c], Xiangsi Wu [a], Yehua Li [a, b], Fang Tang [a, b], Runci Song [a, b], Zhixiong Liu [a], Zeqiang He [a], Xianming Wu [a]

The specific capacity of $ZnMn_2O_4$ is calculated as follows:

$$Specific\ Capacity\ (mAh/g) = \frac{Number\ of\ Electrons \times Faraday's\ Constant \times 1000}{3600 \times Formula\ Weight}$$

$$= \frac{1.6\times10^{-19}C \times 6.022\times10^{23} \times 2 \times 1000}{3600 \times (65.39 + 54.938 \times 2 + 16 \times 4)}$$

$$= 224\ mAh/g$$

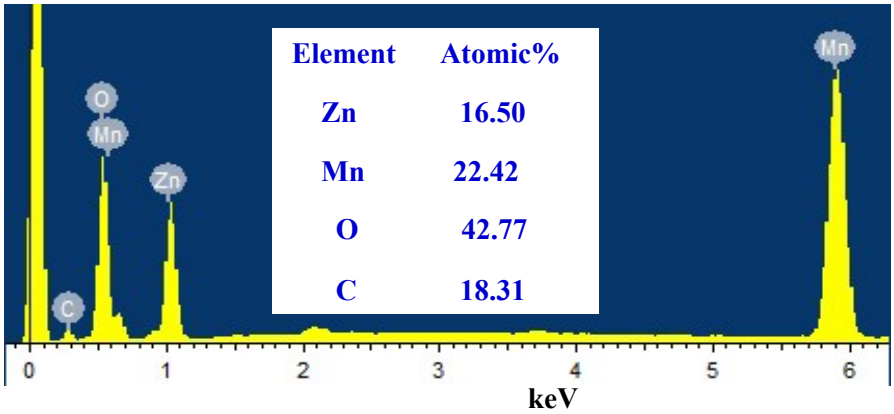

Figure SI-1 EDS of as-prepared $ZnMn_2O_4$

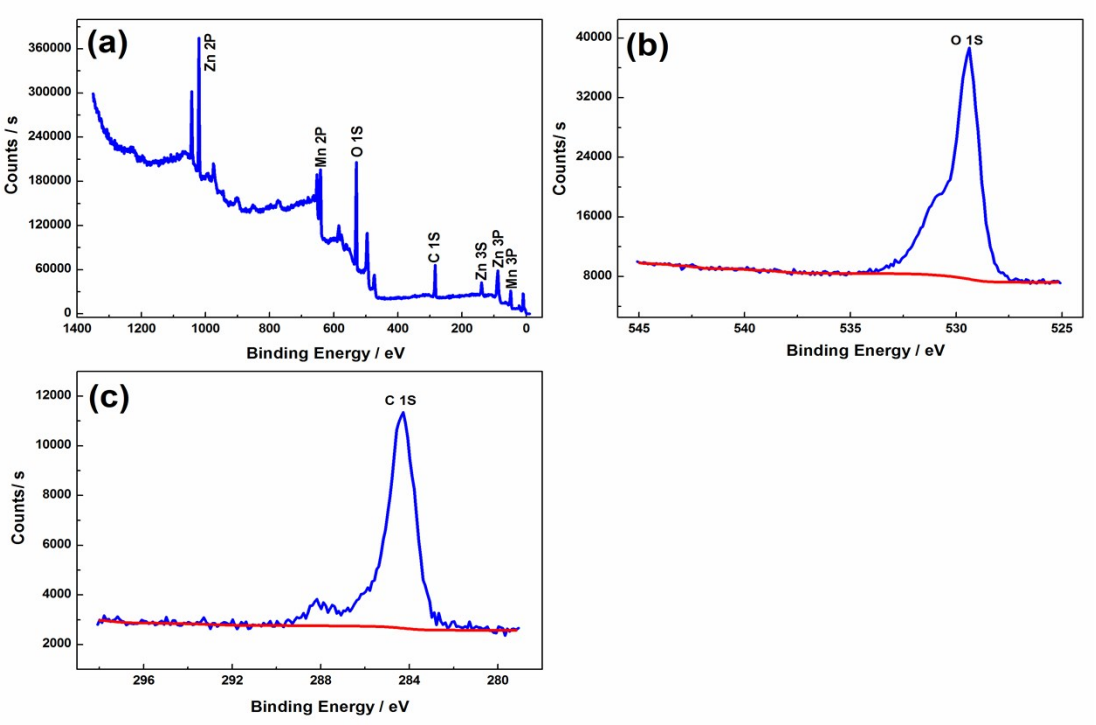

Figure SI-2 XPS spectra of the $ZnMn_2O_4$ samples: (a) survey spectrum; (b) O 1s spectrum; (c) C1s spectrum

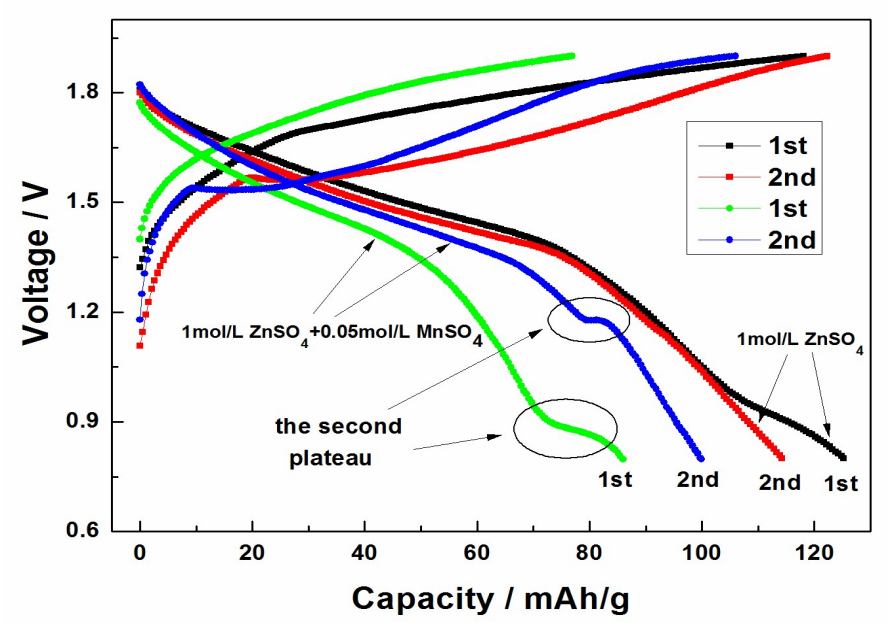

Figure SI-3 The charge/discharge curves of $ZnMn_2O_4$/Zn between 0.8~1.9 V with different electrolytes at 100 mA/g

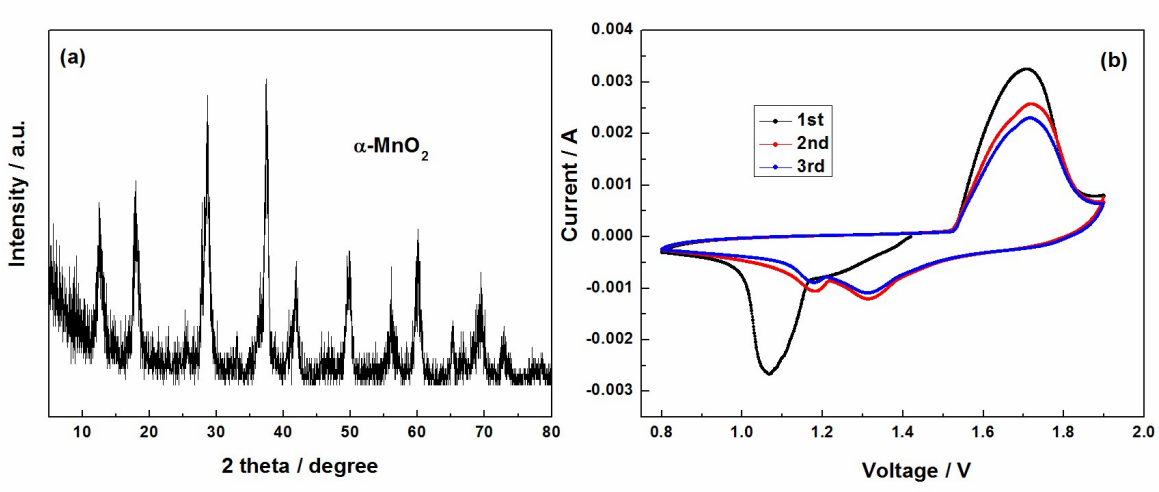

Figure SI-4 XRD of α-MnO_2 and the cyclic voltammetry curve of MnO_2/Zn based on 1mol/L $ZnSO_4$ with 0.05mol/L $MnSO_4$ in the range of 0.8~1.9 V at a scan rate of 1mV/s

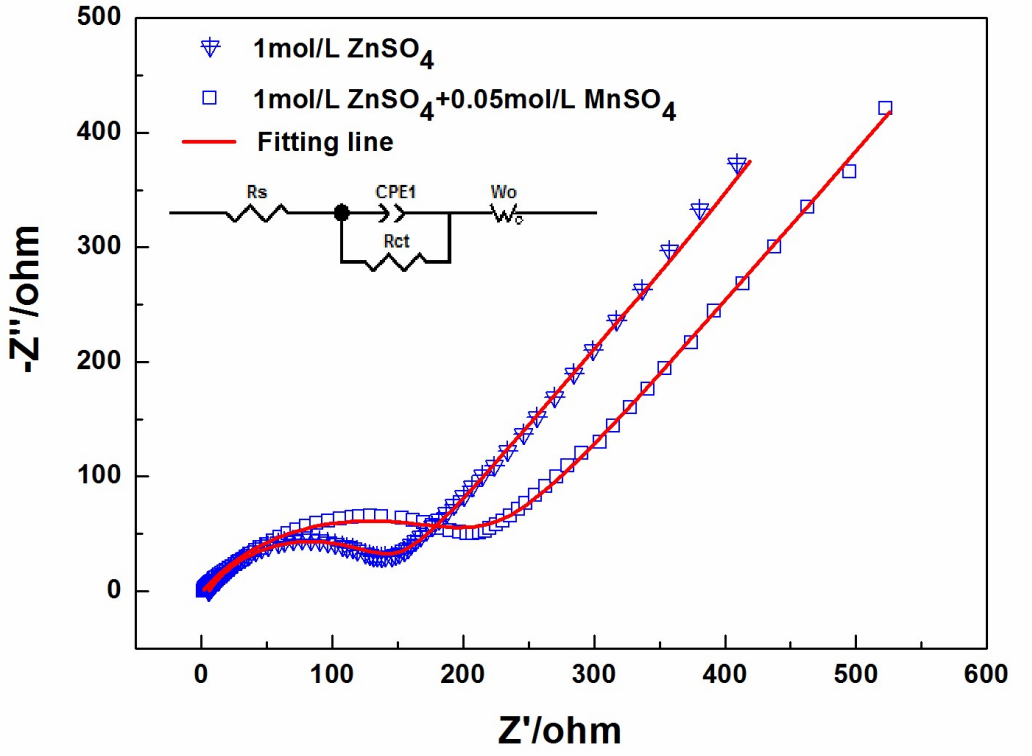

Figure SI-5 EIS spectra and the fitting curves of $ZnMn_2O_4$/Zn before cycling at 100 mA/g

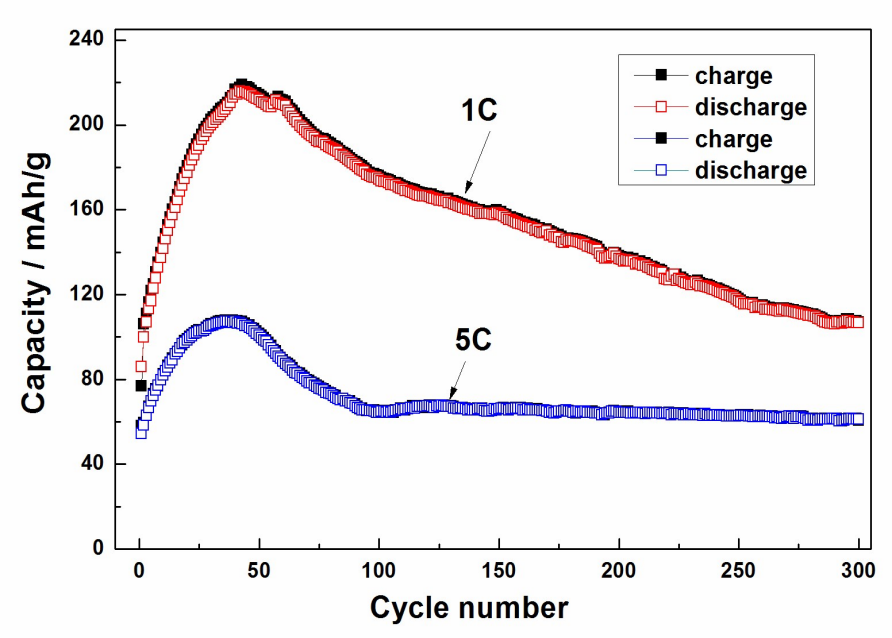

Figure SI-6 The cycling performance of $ZnMn_2O_4$/Zn at different C-rates

A typical cyclic voltammetry curve of Zn^{2+}/Zn half-cell between -0.3～-1.5 V is shown in figure SI-7, and there is an inverted crossover "8" shape along the arrow direction. However, it can be noted that after adding 0.05 mol/L $MnSO_4$ into 1mol/L $ZnSO_4$, the dissolution potential peak is decreased from -1.365 V to -1.372 V in figure SI-7 although the initial coulombic efficiency is decreased a little, demonstrating that $MnSO_4$ decreased the overpotential and facilitated Zn dissolution much easier. As can be seen from figure SI-8 that the deposition/dissolution curves nearly overlap with the cycle number increasing and there is no hydrogen evolution, indicating the good cycleability and high coulombic efficiency of anode.

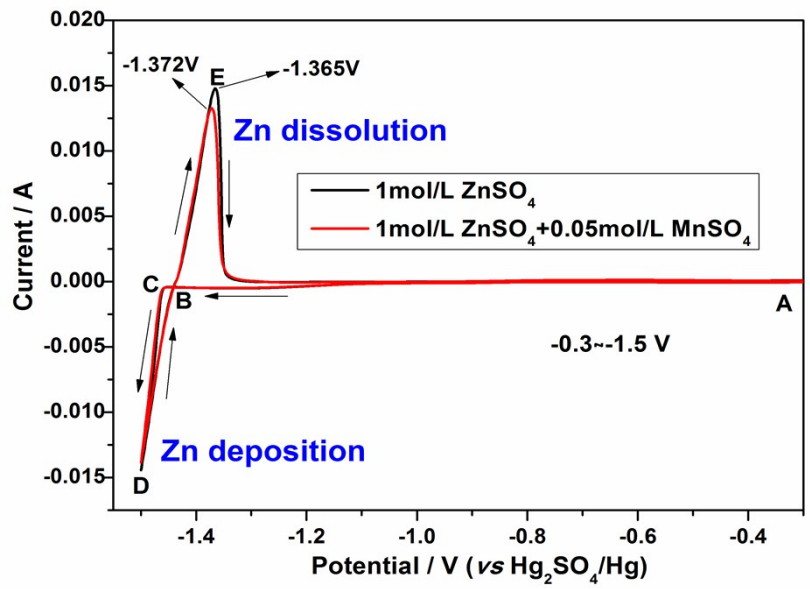

Figure SI-7 The initial deposition-dissolution process of zinc ion at a scan rate of 1 mV/s in different electrolyte

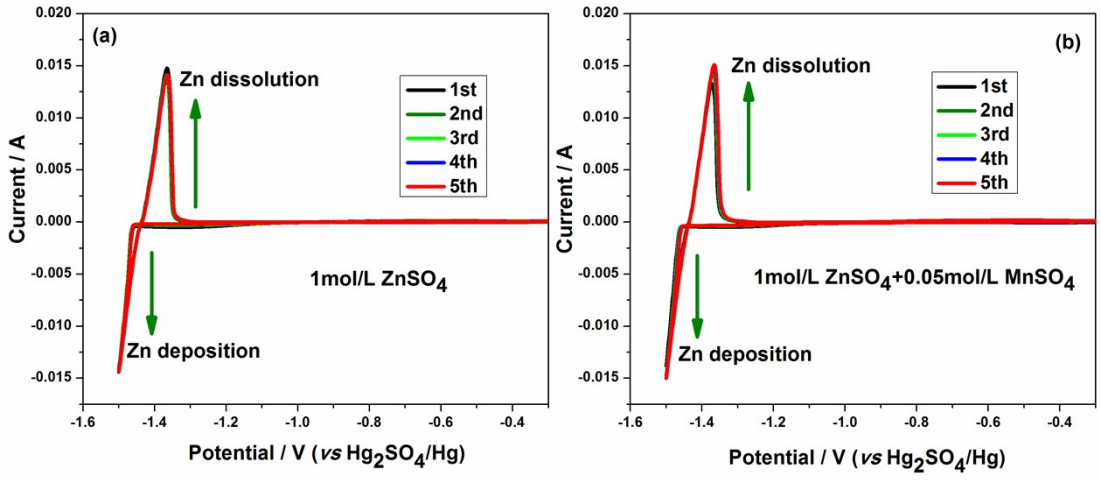

Figure SI-8 The deposition-dissolution process of zinc ion at a scan rate of 1 mV/s in different electrolyte (a, 1mol/L $ZnSO_4$; b, 1mol/L $ZnSO_4$+0.05mol/L $MnSO_4$)

The diffusion kinetics of electrode based on the cyclic voltammetry at different scan rates were analyzed, which can be seen in figure SI-9. Compared figure SI-9 a with figure SI-9 c, after adding $MnSO_4$ into 1mol/L $ZnSO_4$, the polarization phenomenon is decreased, which is consistent with the deposition/dissolution process of Zn^{2+} in different electrolyte in figure SI-7. Notably, the two separate peaks are more obvious after adding $MnSO_4$. It is well known that the

relationship between peak currents and scan rates indicates the different electrochemical reaction characteristics, including solid phase diffusion-controlled or surface-confined charge-transfer processes. As shown in figure SI-9 b and figure SI-9 d, there is a linear relationship between cathodic/anodic current peak and square root of scan rate, demonstrating the diffusion-controlled behavior. According to the Randle-Sevcik equation, $i_p=2.69\times105n^{3/2}AD^{1/2}v^{1/2}C_0$ (25 °C), where i_p is the peak current (mA), n is the number of electrons per reaction species, A is the surface area of the electrode (with the geometric area of the electrode,1.5385 cm^2, used for simplicity in this work), D is the diffusion coefficient of Zn^{2+} (cm^2/s), v is the scan rate (V/s), C_0 is the concentration of zinc ion (0.0436 mol/cm^3, calculated by the cell parameters and cell volume), the slopes can be obtained in figure SI-9 b and figure SI-9 d. The calculated Zn^{2+} diffusion coefficients in different electrolyte are 1.36×10^{-7} cm^2/s, 1.53×10^{-6} cm^2/s, respectively, indicating the higher ion diffusion behavior for the zinc ion aqueous battery. What's more, it is higher after adding $MnSO_4$ into 1mol/L $ZnSO_4$ than that without additive, which will show much better electrochemical performances for the former than that of the latter.

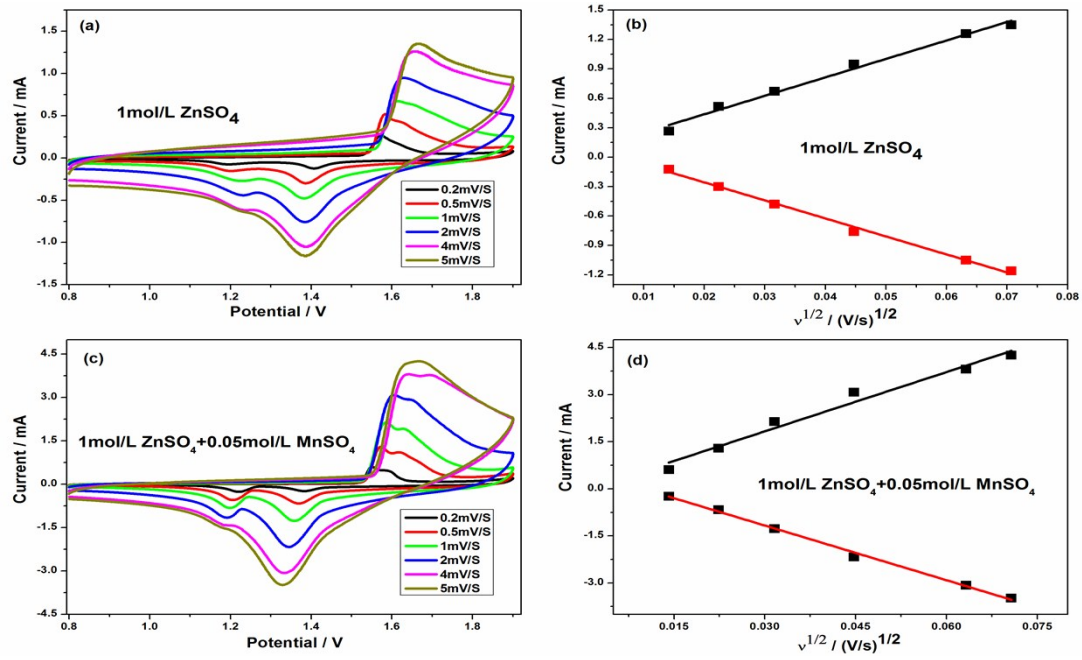

Figure SI-9 (a, c) the cyclic voltammograms of as-prepared $ZnMn_2O_4$ at different scan rates and (b, d) the relationships between the peak current and square root of scan rate in the main cathodic and anodic processes

Table SI-1 Comparison of electrochemical properties of different cathode materials for ZIBs

Samples	Electrolyte	Cycling performance	Ref.
α-MnO_2	1 M $ZnSO_4$	100 mAh g^{-1} at 630 mA g^{-1} with 76% capacity retention after 100 cycles	1
rod-like MnO_2/CNT	2 M $ZnSO_4$+0.5 M $MnSO_4$	100 $mAhg^{-1}$ at 5 A g^{-1} after 500 cycles	2
α-MnO_2 nanorod	1 M $ZnSO_4$	147 mAh·g^{-1} at 83 mAg^{-1} with 63% capacity retention after 50 cycles	3
α-MnO_2 nanorod	1 M $ZnSO_4$	140 mAh g^{-1} at 42 mA g^{-1} with 70% capacity retention after 30 cycles	4
α-MnO_2 nanorod	1 M $ZnSO_4$	104 mAh g^{-1} at 83 mA g^{-1} with 38.5% capacity retention after 75 cycles	5
α-MnO_2 nanorod	2 M $ZnSO_4$+ 0.1 M $MnSO_4$	260 mAh g^{-1}at 308 mA g^{-1} after 60 cycles	6
ZnHCFs	1 M $ZnSO_4$	49.7 mAh g^{-1} at 60 mA g^{-1} with 76% capacity retention after 100 cycles	7
ZnHCFs	1 M $ZnSO_4$	47.4 mAh g^{-1} at 300 mA g^{-1} with 80% capacity retention after 200 cycles	8
$Na_3V_2(PO_4)_3$	0.5M $Zn(CH_3COO)_2$	97 mAh g^{-1} at 0.5C with 74% capacity retention after 100 cycles	9
Spinel-$ZnMn_{1.86}O_4$	3 M $Zn(CF_3SO_3)_2$	80 mAh g^{-1} at 500 mA g^{-1} with 94% capacity retention after 500 cycles	10
Spinel $ZnMn_2O_4$	1 M $ZnSO_4$+0.05M $MnSO_4$	106.5 mAh g^{-1} at 100 mA g^{-1} with 123.87% capacity retention after 300 cycles	This work

Table SI-2 Impedance parameters of equivalent circuit of $ZnMn_2O_4$/Zn

No.	Electrolyte	Rs (ohm)	Rct (ohm)
1#	1mol/L $ZnSO_4$	5.599	138.4
2#	1mol/L $ZnSO_4$+0.05mol/L $MnSO_4$	1.265	214.5

[1] C.J. Xu, B.H. Li, H.D. Du, F.Y. Kang. Angew. Chem., 2012, 124, 957.

[2] D.W. Xu, B.H. Li, C.G. Wei, Y.B. He, H.D. Du, X.D. Chu, X.Y .Qin, Q.H. Yang, F.Y. Kang. Electrochim. Acta, 2014, 133: 254.

[3] M.H. Alfaruqi, J. Gim, S.J. Kim, J.J. Song, J. Jo, S.H. Kim, V. Mathew, J. Kim. J. Power Sources, 2015, 288: 320.

[4] B. Lee, H.R. Li, H. Kim, K.Y. Chung, B.W. Cho , S.H. Oh. Chem. Commun. 2015, 51, 9265.

[5] M.H. Alfaruqi, S. Islam, J. Gim, J.J. Song, S.J. Kim, D.T. Pham, J. Jo, Z.L. Xiu, V. Mathew, J. Kim. Chem. Phys. Lett., 2016, 650: 64.

[6] H.L. Pan, Y.Y. Shao, P.F. Yan, Y.W. Cheng, K.S. Han, Z.M. Nie, C.M. Wang, J.H. Yang, X.L. Li, P. Bhattacharya, K.T. Mueller, J. Liu. Nat. Energy, 2016, 1:16039.

[7] L.Y. Zhang, L. Chen, X.F. Zhou, Z.P. Liu. Adv. Energy Mate,r. 2015, 5(2):1400930.

[8] L.Y. Zhang, L. Chen, X.F. Zhou, Z.P. Liu. Scientific Reports., 2016, 5:18263.

[9] G.L. Li, Z. Yang, Y. Jiang, C.H. Jin, W. Huang, X.L. Ding, Y.H. Huang. Nano Energy, 2016, 25: 211.

[10] N. Zhang, F.Y. Cheng, Y.C. Liu, Q. Zhao, K.X. Lei, C.C. Chen, X.S. Liu, J. Chen. J. Am. Chem. Soc., 2016, 138 (39):12894.